Brownian Ratchets: Molecular Separations in Lipid Bilayers Supported on Patterned Arrays

Alexander van Oudenaarden and Steven G. Boxer*

Brownian ratchets use a time-varying asymmetric potential that can be applied to separate diffusing particles or molecules. A new type of Brownian ratchet, a geometrical Brownian ratchet, has been realized. Charged, fluorescently labeled phospholipids in a two-dimensional fluid bilayer were driven in one direction by an electric field through a two-dimensional periodic array of asymmetric barriers to lateral diffusion fabricated from titanium oxide on silica. Diffusion spreads the phospholipid molecules in the orthogonal direction, and the asymmetric barriers rectify the Brownian motion, causing a directional transport of molecules. The geometrical ratchet can be used as a continuous molecular sieve to separate mixtures of membrane-associated molecules that differ in electrophoretic mobility and diffusion coefficient.

Thermal fluctuations cause particles to move randomly in solution, giving rise to Brownian motion. Brownian particles, when subjected to a spatially asymmetric periodic potential, can undergo net directional motion even if the spatially averaged force is zero. This phenomenon, usually referred to as a Brownian ratchet, has attracted great interest, largely theoretical, from diverse areas of science and technology. Feynman gave a beautiful example in which a mechanical ratchet and pawl subjected to thermal fluctuations are considered to demonstrate the impossibility of violating the second law of thermodynamics (*1*). Brownian ratchets and fluctuation-driven transport are now being considered in the context of biological systems, such as molecular motors, ion pumps, and for the design of biomolecular sieves [for recent reviews see (*2*) and references therein]. We report the experimental realization and characterization of a particular type of Brownian ratchet, a geometrical Brownian ratchet, by using a two-dimensional (2D) fluid lipid bilayer membrane on a patterned solid support.

Most theoretical studies have focused on one-dimensional (1D) systems in which Brownian particles are subjected to a spatially asymmetric periodic potential that is switched on and off as a function of time (*3*). When the potential is switched on, the Brownian particles are driven to the minimum of the spatially periodic potential, whereas the Brownian particles can freely diffuse when the spatial potential is switched off. This gives rise to a net directional motion in one dimension, and the rectifying mechanism of the Brownian ratchet can be used to separate Brownian particles (*4*). A few experiments (*5, 6*) have been performed to test the theoretical predictions. In the geometrical or steric Brownian ratchets (*7–9*), the motion of Brownian particles is constrained by a 2D periodic array of steric barriers. The particles are driven in one direction by a time-independent potential gradient in contrast to a 1D Brownian ratchet, and diffusion spreads the particles out along the orthogonal direction. Diffusion is strongly affected by the asymmetric geometry of the steric barriers. We fabricated such a Brownian ratchet with a lipid bilayer supported by a glass substrate and patterned with microfabricated diffusion barriers. This system provides a truly 2D fluid of Brownian particles and has potential applications in separation of membrane-associated molecules and assemblies.

The principle and our implementation of the geometrical Brownian ratchet are illustrated in Figs. 1 and 2. Negatively charged molecules, in this case a small fraction of fluorescently labeled lipids with negatively charged head groups, are injected at the upper left entrance of the array defined by patterned diffusion barriers highlighted in blue. This is accomplished by application of an electric field, E, applied along the negative y axis and parallel to the plane of the supported membrane. The field exerts an electrophoretic force on the molecules that results in drift velocity $v_y = \mu E$ in the positive y direction (μ is the electrophoretic mobility). Because of the small entrance, the initial concentration profile, shown in red, is highly peaked. Between the spatial coordinates $y = 0$ and $y = y_1$ (Fig. 1) the molecules can diffuse freely between $x = 0$ and $x = x_0$. Between $y = y_1$ and $y = y_2$ diffusion is bounded by diffusion barriers. At $y = y_1$, the broadened concentration profile is cut into two fractions. One fraction, $1 - P$, drifts under the influence of E to the entrance of cell (0,1); the remaining fraction P that drifts to the entrance of neighboring cell (1,1) can be estimated by (*6, 9*):

$$P = \frac{1}{2}\,\mathrm{erfc}\left(\frac{x_b}{2}\sqrt{\frac{v_y}{y_b D}}\right) \approx \frac{1}{2}\exp\left(-\frac{x_b^2}{2y_b}\frac{v_y}{D}\right) \quad (1)$$

where x_b and y_b are determined by the geometry of the cell (Fig. 1), and D is the diffusion coefficient of the molecules. The complement of the error function (erfc) can be approximated by the exponential function. There is a close resemblance between the more common time-dependent Brownian ratchets (*2–6*) and the geometrical Brownian ratchets (*7–9*). In a time-dependent Brownian ratchet, diffusing molecules are subjected to a 1D asymmetric potential that is periodically switched on and off. The 2D geometrical Brownian ratchet is converted into a 1D time-dependent Brownian ratchet when the spatial y coordinate is interpreted as a temporal coordinate, $t = y/v_y$.

We used a lipid bilayer membrane of phospholipid molecules that was supported

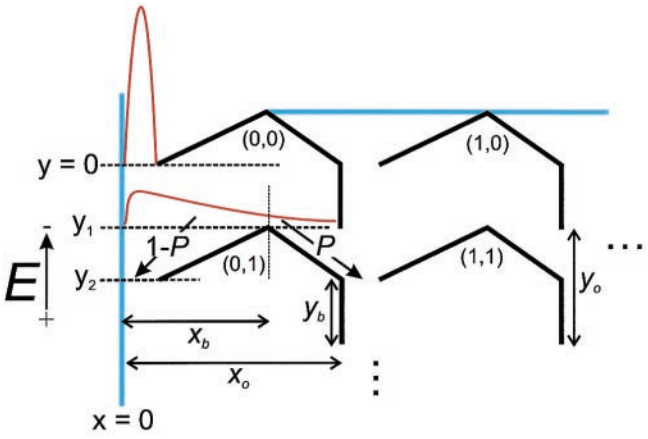

Fig. 1. Sketch of the layout of the geometrical Brownian ratchet projected into the plane of the glass support. Blue lines depict the Ti oxide diffusion barriers bordering the ratchet and defining the entrance in the upper left; black lines are the asymmetric Ti oxide diffusion barriers that create the ratchet. A fluid lipid bilayer is assembled on the open surface but not on the barriers. Negatively charged and fluorescently labeled lipid molecules (red concentration profile) enter at the upper left under the influence of the applied electric field E, which is parallel to the membrane surface. They encounter successive asymmetrical barriers to their lateral mobility and are sieved as indicated.

Department of Chemistry, Stanford University, Stanford, CA 94305–5080, USA.

*To whom correspondence should be addressed. E-mail: sboxer@stanford.edu

by a glass microscope coverslip and patterned with Ti-oxide diffusion barriers (Fig. 2) (*10, 11*). A supported lipid bilayer forms spontaneously in the presence of a hydrophilic surface such as oxidized Si or glass (*12–16*) and is separated from the solid support by a 1-nm-thick water layer (*17*). The supported lipid bilayer undergoes a phase transition from a solid gel phase at low temperature to a liquid phase at higher temperature. In the liquid phase, phospholipid molecules can freely diffuse within each leaflet of the bilayer over macroscopic distances, and the supported lipid membrane retains its uniformity and fluidity for weeks so long as it is hydrated (*18*). The lateral fluidity of the supported membrane is strongly affected by the electrostatic and chemical properties of the substrate material. The membrane is immobile or absent on most metals and metal oxides, which allows us to use the latter as effective barriers to lateral lipid diffusion (*18*).

Membranes were assembled on the clean patterned surface by vesicle fusion (*12–15*). The electrophoresis cell is essentially as described in (*15*). By passing a current through thin Pt electrodes far removed from the ratchet assembly, a tangential electric field parallel to the membrane surface up to 160 V/cm can be applied. Three different unit cell geometries were studied. The geometrical parameter x_b (Fig. 1) is 7, 10, and 13 μm for samples A, B, and C, respectively, whereas y_b = 1 μm for all three samples. The period of the array in the x and y directions (x_o and y_o) is always 1 μm longer than x_b and y_b, respectively. These dimensions were chosen because they are compatible ($P \approx 0.05$ to 0.4) with the value of v_y and D for dye-labeled lipids [see below and (*15*)]. The Ti oxide lines were 200 nm wide and 25 nm high (*18*).

To explicitly demonstrate the effect of the geometrical Brownian ratchet, we have plotted and compared the fluorescence intensity of singly charged 1,2-dipalmitoyl-*sn*-glycero-3-phosphoethanolamine-*N*-(7-nitro-2-1,3-benzoxadiazol-4-yl) (NBD-PE)-labeled lipids (*12*) as a function of x and y for a sample containing no asymmetric cells (Fig. 3A) and for a geometrical Brownian ratchet (Fig. 3B). We obtained similar results when we labeled the lipids with Texas Red, which also has a net single negative charge. In this experiment, the electric field E = 80 V/cm was applied in the negative y direction and exerted an electrophoretic force on the negatively charged lipids (1 mol% of the lipids in the bilayer) in the positive y direction. The data in Fig. 3 were taken after 2 hours of electrophoresis. After 2 hours, all the labeled lipids that were in the geometrical ratchet when the field was switched on have drifted out of the ratchet area, so the pattern of fluorescence shown in Fig. 3 is solely due to new lipids that were injected in the upper left entrance of the sample. At y = 0 a peak in fluorescence intensity was observed at x = 0 because the charged lipids were injected into the sample at this location. In the absence of the geometrical Brownian ratchet (Fig. 3A), the concentration peak broadened as it drifted in the y direction. The position of the fluorescence maximum did not shift from x = 0, as expected for simple unrestricted diffusion. However, in the presence of asymmetric diffusion barriers, a completely different behavior was observed (Fig. 3B). For increasing y (now expressed in unit cell number), the intensity profile broadens and the maximum fluorescence intensity shifts toward larger x. The data in Fig. 3B provide an experimental demonstration of a geometrical Brownian ratchet: the charged molecules move in the direction that is perpendicular to the applied force. From the shift of the fluorescence maximum as a function of y, the fraction of molecules P (Eq. 1) that branched to the next cell can be determined experimentally. After 50 cells in the y direction, the fluorescence maximum shifted about 14 cells in the x direction, which corresponds to $P \approx 14/50 \approx 0.28$. By using Eq. (1) and the geometrical parameters x_b = 10 μm and y_b = 1 μm, $v_y/D \approx 0.007$ μm^{-1} is determined.

Four epifluorescence photographs of geometrical ratchets are shown in Fig. 4. In Fig. 4A, sample B is shown at E = 80 V/cm. A fluorescence intensity plot of this experiment is shown in Fig. 3B. Note that Fig. 4A was taken with a ×10 objective (note the optical diffraction off the grating due to the ratchet structure), whereas B to D were taken with a ×4 objective. The result after 2 hours of electrophoresis in the same sample but at twice the applied field strength (E = 160 V/cm), which increased v_y but did not affect D, is shown in Fig. 4B. Because the molecules are drifting at a greater velocity in the y direction, the probability of branching to a neighboring cell in the x direction is significantly smaller, so the fluorescence profile is considerably steeper in the y direction. Analysis of the slope of the bright fluorescence line in Fig. 4B leads to $P \approx 0.075$ for E = 160 V/cm, which corresponds to $v_y/D \approx 0.04$ μm^{-1}. Interestingly, doubling the external field does not result in a doubling of the v_y/D ratio. This discrepancy can be due to a nonlinearity between v_y and E or to the dominant effect of diffusion at small v_y. At small fields lipids can diffuse past more than one asymmetric barrier in the x direction. In this case Eq. (1) is not valid (*8, 9*).

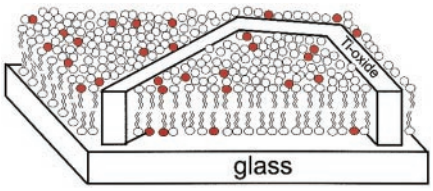

Fig. 2. Schematic perspective diagram of a fluid lipid bilayer on a glass support patterned with a Ti oxide line whose projection onto the surface is shown in black lines in Fig. 1. The Ti oxide lines provide the barriers for the lateral diffusion and mobility of the lipids illustrated in Fig. 1. The bilayer is separated from the glass support by an ~1-nm-thick water layer; the bilayer thickness is ~5 nm. Most of the lipids are neutral and diffuse freely but are not affected by the applied electric field; 1 mol% of the lipid headgroups have a fluorescent label (indicated schematically by red), making the lipids negatively charged. Note that the sketch is not to scale as the barrier is ~25 nm high and 200 nm wide, and the membrane-barrier interface is not characterized at the molecular scale.

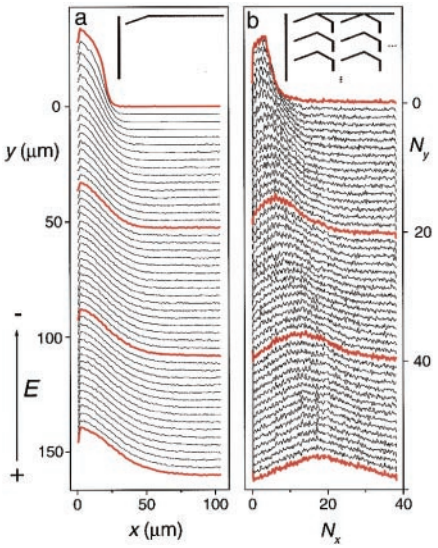

Fig. 3. (**a**) Fluorescence intensity as a function of x and y in units of micrometers for a sample containing no asymmetric cells but with the outer boundaries (illustrated schematically). (**b**) Fluorescence intensity as a function of N_x and N_y in units of the number of cells in x and y directions for sample B (x_b = 10 μm, y_b = 1 μm) for E = 80 V/cm after 2 hours of electrophoresis.

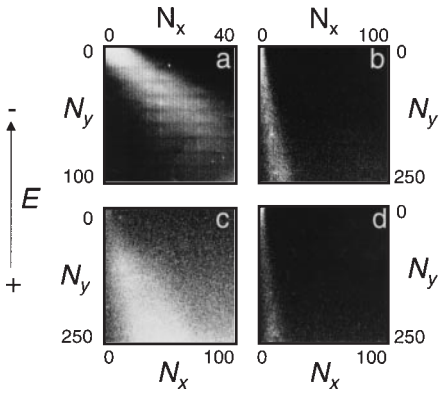

Fig. 4. Epifluorescence photographs after 2 hours of electrophoresis. (**a**) Sample B (x_b = 10 μm), E = 80 V/cm; (**b**) sample B (x_b = 10 μm), E = 160 V/cm; (**c**) sample A (x_b = 7 μm), E = 160 V/cm; (**d**) sample C (x_b = 13 μm), E = 160 V/cm.

The geometrical parameters x_b and y_b should also strongly affect the branching probability P. To explore the influence of the geometry of the cell, three different geometrical ratchets were fabricated and characterized. In Fig. 4 (C and D) epifluorescence photographs of samples A ($x_b = 7$ μm) and C ($x_b = 13$ μm) are shown, respectively, for $E = 160$ V/cm. For samples A and C, P was 0.22 and 0.035, respectively, which results in $v_y/D \approx 0.03$ and 0.04 μm^{-1}, respectively. These values are consistent with the previous observed v_y/D ratios of sample B by using Eq. (1). The measured v_y/D values are comparable to previously measured values extracted from electric field-induced concentration gradients (*15*).

The geometrical Brownian ratchet can also be used to separate mixtures of different lipids or, in principle, membrane-associated proteins that have different values of v_y/D. As a proof of concept, a separation of the two fluorescently labeled lipids, *N*-(Texas Red sulfonyl)-1,2-dihexadeconyl-*sn*-glycero-3-phosphoethanolamine (Texas Red-DHPE), which has a single negative charge, and 1,2-dioleoyl-*sn*-glycero-3-phospho-L-serine-*N*-(7-nitro-2-1,3-benzoxadiazol-4-yl) (NBD-PS), which has a double negative charge, is shown in Fig. 5. The symbols in Fig. 5 denote the maximum in fluorescence intensity. We find $P \approx 0.22$ and P ≈ 0.16, which leads to $v_y/D \approx 0.012$ μm^{-1} and $v_y/D \approx 0.020$ μm^{-1} for Texas Red-DHPE and NBD-PS, respectively. The v_y/D ratio of NBD-PS is greater because of its double negative charge, which increases the electrophoretic force. Experiments that monitor the drift of a concentration front as a function of time (*14*) showed that v_y of NBD-PS is about 50% greater than v_y of Texas Red-DHPE at $E = 80$ V/cm. These values are consistent with the observed v_y/D ratios, assuming that the diffusion coefficients of the two different lipids are similar. The separation at $N_y = 60$ is only partial because the bands of the two lipids overlap. However, the resolution of the geometrical Brownian ratchet increases with time because the separation between the bands scales with N_y, whereas the width of a band scales only with $(N_y)^{1/2}$ (*8, 9*).

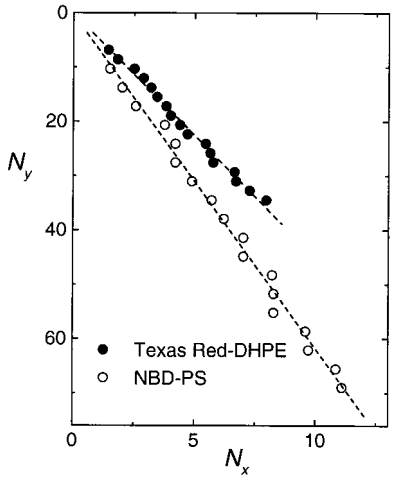

Fig. 5. Maximum of fluorescence intensity as a function of number of cells in *x* and *y* directions for Texas Red-DHPE and NBD-PS. Data were taken after 2 hours of electrophoresis at $E = 80$ V/cm.

The potential advantages of this separation technique over traditional techniques are that membrane-associated components could be separated in their native environment and the separations are continuous. In addition, the motion of membrane-associated molecules in the ratchet is a sensitive probe of their mobility. This can be affected by association or clustering within the membrane, binding to molecules in solution, or a combination—for example, receptor association mediated by binding a hormone (*19*). Many different kinds of lipids, including glycolipids (*20*), an important class of cell surface receptors, are mobile in membranes on solid supports as members of the large class of proteins that are anchored to membranes by lipids such as glycan phosphatidyl-inositol (GPI)–linked proteins (*21*). Simple transmembrane peptides such as gramicidin are also mobile (*22*); however, most integral membrane proteins studied to date are not mobile on solid supports. Many strategies are being developed to tether membranes to solid supports in a way that may maintain the lateral mobility of integral membrane proteins (*22, 23*) and that are, in principle, compatible with the patterning and electrophoresis required to assemble a ratchet. Integral membrane proteins are a very large, important, and typically difficult class of proteins to work with; thus methods to achieve separations and characterization in their native environment should be useful.

References and Notes

1. R. P. Feynman *et al.*, *The Feynman Lectures on Physics* (Addison-Wesley, Reading, MA, 1966), vol. 1, pp. 46-1–46-9.
2. R. D. Astumian, *Science* **276**, 917 (1997); _____ and F. Moss, *Chaos* **8**, 533 (1998).
3. M. O. Magnasco, *Phys. Rev. Lett.* **71**, 1477 (1993); R. D. Astumian and M. Bier, *ibid.* **72**, 1766 (1994).
4. A. Ajdari and J. Prost, *C. R. Acad. Sci. Ser. II* **315**, 1635 (1992).
5. J. Rousselet *et al.*, *Nature* **370**, 446 (1994); L. P. Faucheux and A. Libchaber, *J. Chem. Soc. Faraday Trans.* **91**, 3163 (1995).
6. L. P. Faucheux *et al.*, *Phys. Rev. Lett.* **74**, 1504 (1995).
7. G. W. Slater, H. L. Guo, G. I. Nixon, *ibid.* **78**, 1170 (1997).
8. D. Ertas, *ibid.* **80**, 1548 (1998).
9. T. A. J. Duke and R. H. Austin, *ibid.*, p. 1552 (1998); I. Derényi and R. D. Astumian, *Phys. Rev. E* **58**, 7781 (1998).
10. The pattern for the geometrical Brownian ratchet was defined by electron beam lithography. First a 200-nm-thick poly(methyl methacrylate) resist layer was spun onto a glass microscope coverslip, which was subsequently baked and coated with an 80-nm-thick layer of a conducting polymer (*11*) to prevent charging of the insulating glass coverslip during exposure. After electron beam exposure, the conducting polymer was dissolved in water and the resist was developed. Finally a 30-nm film of Ti was evaporated onto the coverslip. After liftoff, the Ti was oxidized for several hours at 400°C. Before deposition of the lipid bilayer, the patterned coverslips were rinsed for 15 min in hot 7X detergent (ICN Biochemicals, Aurora, OH) and then rinsed with purified water. The coverslips were dried under a nitrogen stream and then heated to 400°C for 4 hours.
11. T. Shimizu *et al.*, *Synth. Met.* **85**, 1337 (1997).
12. The supported lipid bilayer was formed by fusion of small unilamellar vesicles (SUVs) with the patterned coverslips. The SUVs were prepared according to the Barenholtz procedure; for a detailed description of the procedure see (*13–15*). The SUVs consist of 99 mol% of the neutral (zwitterionic) phospholipid L-α-phosphatidylcholine (egg-PC; Avanti Polar Lipids, Alabaster, AL) and 1 mol% of the negatively charged, labeled lipids. The bilayer was produced by putting the patterned coverslip on a 70-μl drop of small unilamellar vesicles in a petri dish, which was then filled with purified water and shaken gently to remove nonfused vesicles. Under water, a clean nonpatterned coverslip was placed at the side of the bilayer and this sandwich was transferred to an electrophoresis cell. The electrophoresis cell consists of two reservoirs filled with purified water and each contains a thin platinum electrode (*15*). The sandwich was placed between the two reservoirs; the water sandwiched between the coverslips provides electrical contact between the two Pt electrodes. All experiments were performed at room temperature. The diffusion and drift of the charged lipids were monitored with a Nikon E800 epifluorescence microscope with a ×4 or ×10 objective and a charge-coupled device camera. The negatively charged fluorescent probes were covalently attached to the phospholipid headgroup (Texas Red-DHPE from Molecular Probes, Eugene, OR; NBD-PE and NBD-PS from Avanti Polar Lipids, Alabaster, AL). The labeled lipids NBD-PE and Texas Red–DHPE carry a net single negative charge, whereas NBD-PS has a double negative charge.
13. Y. Barenholtz *et al.*, *Biochemistry* **16**, 2806 (1977).
14. J. Salafsky, J. T. Groves, S. G. Boxer, *ibid.* **35**, 14773 (1996).
15. J. T. Groves and S. G. Boxer, *Biophys. J.* **69**, 1972 (1995).
16. A. A. Brian and H. M. McConnell, *Proc. Natl. Acad. Sci. U.S.A.* **81**, 6159 (1984); E. Sackmann, *Science* **271**, 43 (1996).
17. T. M. Bayerl and M. Bloom, *Biophys. J.* **58**, 357 (1990); S. J. Johnson *et al.*, *ibid.* **59**, 289 (1991); B. W. König *et al.*, *Langmuir* **12**, 1343 (1996).
18. J. T. Groves, N. Ulman, S. G. Boxer, *Science* **275**, 651 (1997); J. T. Groves *et al.*, *Langmuir* **14**, 3347 (1998). Metal oxides such as Al_2O_3 and TiO_2 are barriers to lateral diffusion because of their surface properties and not their topography. If similar structures are fabricated from SiO_2, the membranes are conformal and will follow the contour of corrugated surfaces without disruption.
19. J. A. Wells and A. M. Devos, *Annu. Rev. Biophys. Biomol. Struct.* **22**, 329 (1993).
20. L. Kung, X. Song, B. Swanson, S. G. Boxer, unpublished data.
21. J. T. Groves, C. Wülfing, S. G. Boxer, *Biophys. J.* **71**, 2716 (1996). The typical drift velocities of GPI-linked proteins are significantly larger than was observed for charged lipids, which facilitates separation and relaxes the need for submicrometer lithography.
22. B. A. Cornell *et al.*, *Nature* **387**, 580 (1997).
23. T. Stora, J. H. Lakey, H. Vogel, *Angew. Chem. Int. Ed. Engl.* **38**, 389 (1999).

24. Supported in part by a grant from the NSF Biophysics Program, by the Materials Research Science and Engineering Center Program of the NSF under award DMR-9808677, and by a grant from SmithKline Beecham. A.v.O. acknowledges the Netherlands Organization for Scientific Research (NWO) for financial support. We acknowledge very useful discussions and insights from J. T. Groves in the development of this project and valuable comments and suggestions on the manuscript by R. D. Astumian. The Stanford Nanofabrication Facility is acknowledged for support in fabrication.

26 March 1999; accepted 16 June 1999